Available online at www.sciencedirect.com
SCIENCE DIRECT®
Biochemical and Biophysical Research Communications 329 (2005) 132–139
BBRC
www.elsevier.com/locate/ybbrc

CD83 is a dimer: Comparative analysis of monomeric and dimeric isoforms

Matthias Lechmann[a], Nicole Kotzor[a], Elisabeth Zinser[a], Alexander T. Prechtel[a], Heinrich Sticht[b], Alexander Steinkasserer[a,*]

[a] *University Hospital Erlangen, Department of Dermatology, Hartmannstr. 14, D-91052 Erlangen, Germany*
[b] *University of Erlangen, Institute of Biochemistry, Emil-Fischer-Zentrum, Fahrstraße 17, D-91054 Erlangen, Germany*

Received 19 January 2005

Abstract

Recently, we reported that soluble CD83 has a strong immunosuppressive activity in vitro as well as in vivo. Sequence alignment of CD83 between different species revealed the presence of five cysteines in the extracellular Ig-domain of the protein. This opens up the possibility that four cysteines are involved in the formation of two intramolecular disulfide bonds and a possible involvement of the remaining fifth cysteine in the formation of an intermolecular covalent disulfide bond, leading to the dimerization of the extracellular protein domains. Using recombinant mutational analyses, where the fifth cytosine at amino acid position 129 was mutated to a serine, we could prove that the fifth cysteine residue was indeed necessary for the dimerization. Functional analyses revealed that the mutant protein inhibited almost completely the upregulation of CD83-expression during DC maturation. Furthermore, the functional activity of the mutant protein was investigated using MLR assays and we could show that the mutant soluble CD83 protein inhibited DC-mediated allogeneic T-cell stimulation in vitro.

Keywords: CD83; Dendritic cells; Dimerization; MLR

The human CD83 (hCD83) is a member of the immunoglobulin superfamily. It consists of an extracellular immunoglobulin-like domain, a transmembrane domain, and a 39 amino acid intracellular domain [1,2]. Its extracellular domain is highly glycosylated [3]. The murine CD83 (mCD83) has also been characterized and DNA sequence analyses revealed a 196 amino acid protein including a signal peptide of 21 amino acids, which shares overall 63% amino acid identity with human CD83. Murine CD83 is also a glycoprotein [4,5].

Human CD83 is expressed predominantly on the surface of dendritic lineage cells, including skin Langerhans cells, circulating DC, and interdigitating reticulum cells present in the T-cell areas of lymphoid organs [1,6,7]. After stimulation with inflammatory cytokines, CD83-expression is induced in mature DC together with costimulatory molecules such as CD80 and CD86 [8]. Murine CD83-expression is also strongly upregulated in mature bone marrow-derived DC after stimulation with lipopolysaccharide (LPS) and/or TNF-α [5].

DC are the most potent antigen presenting cells of the immune system. In their immature stage, they sentinel in peripheral tissues. Upon encounter with antigens, like pathogens or tumor antigens, and inflammatory cytokines, they start to mature and change their phenotype and functions. Thereby they migrate to lymphoid organs where they trigger antigen-specific T-cell responses [9–11].

Several viruses such as HSV-1 [12], HIV-1 [13], measle virus [14], vaccinia virus [15,16], and HCMV [17] have been shown to interfere with CD83-expression in

* Corresponding author. Fax: +49 9131 8535799.
E-mail address: alexander.steinkasserer@derma.imed.uni-erlangen.de (A. Steinkasserer).

0006-291X/$ - see front matter © 2005 Elsevier Inc. All rights reserved.
doi:10.1016/j.bbrc.2005.01.114

infected DC, which then consequently also interfered with DC-mediated T-cell stimulation. Furthermore in experiments, where the CD83 mRNA transport from the nucleus into the cytoplasm was specifically inhibited, and thus CD83-expression was blocked, the T-cell stimulatory capacity of these DC was also inhibited [18]. All these reports clearly suggested an important role for CD83 during the induction of immune responses. However, the precise function of CD83 is still unknown.

In this respect, we were able to demonstrate for the first time that a soluble CD83 inhibited DC maturation and furthermore completely blocked DC-mediated T-cell stimulation in vitro [19]. The inhibitory activity of soluble CD83 was confirmed by Scholler et al. [20], whereby anti-tumor responses have been reduced using a CD83-Ig fusion protein. Further analysis regarding the mode of action revealed that soluble CD83 inhibits DC-T-cell clustering, a prerequisite for DC-mediated T-cell stimulation, and very interestingly, a dramatic effect of soluble CD83 on the cytoskeleton of mature DC has been observed [21].

In addition, we investigated the effect of soluble CD83 also in vivo using the murine experimental autoimmune encephalomyelitis (EAE) model, a $CD4^+$ T-cell-mediated autoimmune disorder and model for the early inflammatory stage of human multiple sclerosis. Strikingly, only three injections of soluble CD83 inhibited the paralysis associated with EAE almost completely [22]. This suppressive effect was also long lasting, since mice, in which EAE was induced for a second time, were still protected, while untreated mice were again strongly paralyzed. Furthermore, soluble CD83 strongly reduced the paralysis also in a therapeutic setting [22].

Here we provided evidence that CD83 can form dimers via disulfide bonds. Using mutational analyses the Cys residue at position 129 of the extracellular CD83 domain has been identified to be absolutely necessary for the homodimerization. The mutant CD83 protein which had a cysteine to serine exchange was no longer able to form dimers. Interestingly, functional analyses revealed that the mutant CD83 protein has similar immunosuppressive effects as the wild type CD83 molecule, i.e., it had similar inhibitory effects regarding the CD83-upregulation during DC maturation and completely blocked DC-mediated T-cell stimulation in vitro. Finally, we present a three-dimensional structural model for soluble CD83 which is based on sequence alignment and molecular modeling.

Materials and methods

Sequence alignment and molecular modeling. Information regarding the molecular architecture of CD83 was obtained from sequence and domain database searches using PSI-BLAST [23], Pfam [24], and SMART [25]. Templates of known three-dimensional structure suitable for homology modeling were detected using the SAM-T2K server that relies on hidden Markov models for protein structure prediction [26]. Homology modeling was performed using the SWISS-MODEL server [27] and the results were verified using WHATCHECK [28].

Expression and purification of soluble CD83 (hCD83ext). The extracellular domain of human CD83 (amino acids 20–145) has been subcloned into the pGEX2T vector (Amersham-Pharmacia Biotech, Uppsala, Sweden), expressed, and purified as described in detail before [3]. Shortly, an overnight bacterial culture diluted 1:10 in fresh LB medium supplemented with 100 g/ml ampicillin at a density of 1.0 IPTG was added (final concentration 1 mM) and the culture proceeded for 2 h. The cells were pelleted, resuspended in 10 ml native buffer (140 mM NaCl, 2.7 mM KCl, 10 mM Na_2HPO_4, 1.8 mM KH_2PO_4, 2.6 mM MnCl, 26 mM $MgCl_2$, 1 g/ml leupeptin, 1 g/ml aprotinin, and 1 g/ml DNAse I, pH 7.6) per 500 ml culture and 50 g/ml lysozyme was added. After 30 min incubation on ice, the lysate was spun at 20,000*g*. Capture step: 40 ml supernatant was added to a GSTrap 5 ml column on an ÄKTA Explorer 10 system (Amersham-Pharmacia Biotech). Binding buffer: PBS, pH 7.6. Elution buffer: 50 mM Tris–HCl, pH 8.0, with 5 mM reduced glutathione. Flow rate: 5 ml/min. Chromatographic procedure: 4 CV (column volumes) binding buffer, 40 ml supernatant, 12 CV binding buffer, 5 CV elution buffer, 5 CV 2 N NaCl/PBS, pH 7.6, and 5 CV binding buffer. For buffer exchange, the GST-CD83ext containing elutions were desalted over a HiPrep 26/10 column (Amersham-Pharmacia Biotech). Running buffer: PBS, pH 7.6. Flow rate: 10 ml/min. Then the GST-hCD83ext fusion protein was incubated with thrombin 20 U/ml glutathione–Sepharose matrix at 22 °C for 16 h. To separate the hCD83ext protein from GST, the elution was loaded onto prepacked glutathione–Sepharose 4B columns using the same buffer conditions as in the capture step. Under binding buffer conditions the flow through containing recombinant human CD83ext protein was collected. Polishing step: finally, a preparative gel filtration separation was performed loading the flow through onto a Superdex 200 (26/16) prep grade column on an ÄKTA Explorer 10 system (Amersham-Pharmacia Biotech), running buffer PBS, pH 7.6, flow rate 3 ml/min. The purified CD83ext was concentrated in an Amicon stirred cell (Millipore, Eschborn, Germany) using an Ultracell Amicon YM10 Ultrafiltration disk (Millipore).

Cloning of the mutant hCD83ext in Escherichia coli. The mutant extracellular domain of human CD83 (amino acids 20–145) was PCR-amplified using the following primer set: sense-pGEX2ThCD83, 5′-TCCCCCCGGGAACGCCGGAGGTGAAGGTGGCT-3′ and antisense-CD83extra_mutantCtoS, 5′-AATTAGAATTCTCAAATCTCC GCTCTGTATTTCTTAAAAGTCTCTTCTTTACGCTGTGCAGG GGAT-3′ (MWG-Biotech AG). The antisense primer inserts a g to c nucleotide transversion, which leads to an amino acid exchange of cystidine to serine at the amino acid position 129. The amplified cDNA fragment was subcloned into the *Sma*I and *Eco*RI sites of the expression vector pGEX2T (Amersham-Pharmacia Biotech) resulting in the plasmid pGEX2ThCD83ext_mut129_CtoS and was transformed into the *E. coli* strain BL21(DE3) pLysS (Novagen, Schwalbach, Germany). The correct nucleotide sequence was verified by sequencing.

Expression and purification of hCD83ext_mut_129_CtoS. The mutant protein hCD83ext_mut129_CtoS was expressed in BL21(DE3)-pLysS (Novagen) and purified as described above for hCD83ext.

Generation of human dendritic cells. PBMCs were isolated from leukapheresis preparations by density gradient separation using Lymphoprep (Nycomed Pharma AS, Oslo, Norway). Cells were seeded into cell culture flasks and incubated at 37 °C in 5% CO_2. Incubation of cells was performed in medium which consists of RPMI 1640 (BioWhittaker, Verviers, Belgium) plus 1% glutamine (Sigma–Aldrich, Deisenhofen, Germany), 1% penicillin/streptomycin (Sigma–Aldrich), 1% Hepes (Gibco-BRL, Karlsruhe, Germany), and 1% heat-inactivated (56 °C; 30 min) human plasma. After 1 h of incubation, the non-adherent cell fraction (NAF) was removed and the adherent cells were further incubated for 24 h. The NAF was used in mixed leukocyte reactions. Afterwards, cells were fed with GM-CSF (800 U/ml) (Am-

gen GmbH, München, Germany) and IL-4 (500 U/ml) (Strathmann, Hamburg, Germany), and incubated again for 48 h. Then, cells were fed again with GM-CSF (400 U/ml) and IL-4 (500 U/ml). Forty-eight hours later, these cells were treated with a maturation cocktail composed of GM-CSF (40 U/ml), IL-4 (200 U/ml), IL-1β (1 ng/ml; Sigma–Aldrich), PGE_2 (0.5 μg/ml; Cayman Chemicals, Ann Arbor, MI, USA), and TNF-α (1.25 ng/ml; Boehringer Ingelheim, Vienna, Austria). For the different experiments reported here, the cells were either matured with cocktail alone, with addition of GST (10–15 μg/ml; as a control), or in the presence of either hCD83ext or hCD83ext_mut129_CtoS (10–15 μg/ml). After additional incubation of 24–48 h, those matured DC were harvested and analyzed.

FACS analysis. The maturation and differentiation status of DC was determined by staining for the following surface markers: CD14, CD25, CD40, CD80, CD83, CD86, and MHC II (FITC or PE-conjugated antibodies, BD, Heidelberg, Germany). CCR7 was detected by indirect immunofluorescence using PE-conjugated goat-anti-mouse Ig (BD, Heidelberg, Germany). Staining and washing was performed in phosphate-buffered saline (PBS) (136 mM NaCl, 8 mM Na_2HPO_4, 1.5 mM KH_2PO_4, and 2.7 mM KC1, pH 7.4) supplemented with 1% FCS. Cells were incubated for 30 min on ice with each antibody in the appropriate dilution. After washing once with PBS, samples were analyzed with a FACScan (Becton–Dickinson, Heidelberg, Germany).

SDS–PAGE and immunoblotting analyses. HPLC-purified proteins were separated on 15% sodium dodecyl sulfate (SDS)–polyacrylamide gels and blotted onto nitrocellulose filters. The membranes were blocked with 5% dried milk in TBST (20 mM Tris–HCl, pH 7.5, 150 mM NaCl, and 0.05% Tween 20) for 1 h. Incubation with the monoclonal anti-CD83 antibody (1:100 CD83-1G11) [3] was performed overnight at 4 °C or for 1 h at room temperature in blocking solution. After washing three times with TBST, the filters were incubated for 1 h at RT with a 1:20,000 dilution of the rabbit-anti-rat IgG antibody coupled to horseradish peroxidase (Dianova, Hamburg, Germany). Immunoreactive bands were visualized using an epichemiluminescence Western blotting system (Amersham-Pharmacia Biotech, Freiburg, Germany) according to the manufacturer's protocol.

Surface plasmon resonance (Biacore) analysis. A Biacore X system and CM5 sensor chips (research grade) were used for binding studies (Biacore AB). GST or GST-hCD83ext fusion protein was immobilized on the chip surface using the Biacore GST-kit for fusion capture (Biacore AB) according to the manufacturer's instructions. Proteins were diluted to concentrations between 5 and 10 μg/ml in HBS-EP buffer (10 mM Hepes, pH 7.4, 150 mM NaCl, 3 mM EDTA, and 0.005% polysorbate 20) and captured on the chip at a flow rate of 5 μl/min, until a change of at least 1.000–1.500 resonance units (RU) was detectable. The RU baseline was then allowed to stabilize for at least 15 min. For the determination of interactions, the hCD83ext or hCD83ext_mut129_CtoS proteins were diluted in HBS-EP buffer to a final volume of 80 μl and subsequently injected over both flow cells (flow cell 1: GST; flow cell 2: GST-hCD83ext) at a flow rate of 20 μl/min. The injected proteins were allowed to dissociate from the bound protein during a wash step in which HBS-EP buffer was injected for an additional 60–90 s. To completely remove bound proteins, the chip was regenerated by using the GST-kit regeneration solution capture (Biacore AB) according to the manufacturer's instructions. Upon completion of the binding profiles, the responses from all flow cells were baseline corrected. The response from the reference cell (flow cell 1: GST) was subtracted from the response of flow cell 2 (GST-hCD83ext) to correct for refractive index changes, non-specific binding, and instrument drift. All experiments were performed at RT.

T-cell proliferation assay. The CD4 and CD8 positive (NAF) T-cells were stimulated at different ratios with mature allogeneic DC in a final volume of 200 μl/well RPMI 1640 supplemented with 5% human serum from a single AB donor in 96-well plates. These mixed leukocytes were treated with hCD83ext (10 μg/ml), hCD83ext_mut129_CtoS (10 μg/ml) or left untreated (MOCK) and incubated for 4 days at 37 °C. Then the cells were pulsed with 1 μCi/well [^{3}H]thymidine (Amersham) for 16 h. The culture supernatants were harvested onto glass fiber filters (Printed Filtermat A; Wallac, Turcu, Finland) by using an ICH-110 harvester (Inotech, Dottikon, Switzerland), and [^{3}H]thymidine incorporation was determined using a microplate counter (Wallac).

Results

Sequence alignment and molecular modeling of the CD83 structure

Human and mouse CD83 show a sequence identity of 59% for their extracellular parts. The major difference between hCD83 and mCD83 is an 11-residue deletion comprising residues 65–75 in mCD83 (Fig. 1). Iterative sequence database searches using PSI-BLAST suggest that both molecules represent divergent members of the immunoglobulin (Ig) family. This result is confirmed by Pfam and SMART database searches showing the existence of a domain with an immunoglobulin-fold for hCD83 and mCD83 at high confidence levels. According to the SMART database, the Ig-domain comprises the first 108 and 97 residues of mature hCD83 and mCD83, respectively, and is connected to the transmembrane helix by a linker sequence of yet unknown function.

Human CD83 and murine CD83 contain a total of five cysteine residues at equivalent sequence positions two of which are also highly conserved within the immunoglobulin family. Very recently, a novel member of the CD83 family from the nurse shark *Ginglymostoma cirratum* has been reported (gCD83) which exhibits 30% sequence identity to hCD83 [29]. Interestingly, this protein contains three cysteines, suggesting that an uneven number of cysteines is a common feature for the CD83 family members.

The presence of an uneven number of cysteines in the extracellular CD83 domain suggests that an even number of these cysteines will form intramolecular disulfide bonds, while the remaining cysteine might be involved in intermolecular covalent interactions.

In order to identify the spatial location of the 11-residue deletion present in murine CD83, the three-dimensional structure of human CD83 was modeled using the structure of the Bl-8 Fv fragment (PDB code: Ia6w) as a template, which was identified as the closest homologue of known three-dimensional structure by a SAM-T2K search [26].

The residues corresponding to the insertion present in hCD83 compared to mCD83 are mainly located in the outer strand of a β-sheet (Fig. 2A). As evident from Pfam domain alignments this part of the sequence generally exhibits a considerable variability in sequence length and structure in different members of the Ig family. Molecular modeling of mCD83 based on hCD83 reveals that the Ig-fold can accommodate the 11-residue deletion without changes of the Ig core fold (Fig. 2B).

```
                10        20         30        40        50
                 |         |          |         |         |
hCD83   MSRGLQLLLLSCAYSLAPATP--EVKVACSEDVDLPCTAPWDPQVPY-TVSWVKLLEGGEE

mCD83   MSQGLQLLFLGCACSLAPAMAMREVTVACSETADLPCTAPWDPQLSY-AVSWAKVSESGTE

gCD83   MFHLKKCWFLAVQGLVFVATKSISEVTVKCGEAARLPCKAEYEVGVQYRALSWYKIADDGVG

1a6w                            AELVKPGASVKLSCKASGYTFTSY-WMHWVKQ-RPGRG

        60        70        80          90       100       110
         |         |         |           |         |         |
hCD83   RMETPQEDHLRGQHYHQKGQNGSFDAPNER---PYSLKIRNTTSCNSGTYRCTLQDPDGQRNL

mCD83   SVELPE-----------SKQNSSFEAPRRR---AYSLTIQNTTICSSGTYRCALQELGGQRNL

gCD83   LTGILRKDFRENIVRKYLGFNRSVELASDM---LFSLIIHNVTSEDFGKYQCSMWAPLGKQNR

1a6w    LEWIGRIDPNSGGTKYNEKFKSKATLTVDKPSSTAYMQLSSLTSEDSAVYYCARYDYYGSSYF

     120       130       140
       |         |         |
hCD83   SGKVILRVTGCPAQRKEETFKKYRAEI

mCD83   SGTVVLKVTGCPKEATESTFRKYRAEA

gCD83   QADVDLQEVGILQSKRLG

1a6w    DYWGQGTTVTVSSQQPT
```

Fig. 1. Multiple sequence alignment of the extracellular parts of CD83 from human (hCD83), mouse (mCD83), and *G. cirratum* (gCD83). The first 20 residues, depicted in italic, represent the signal sequence which is absent in the mature protein. The last line represents the sequence of the Bl-8 Fv fragment (PDB code: 1a6w) which served as a template for modeling of hCD83. The alignment was generated by ClustalW and SAM-T2K. Cysteine residues are shown in bold.

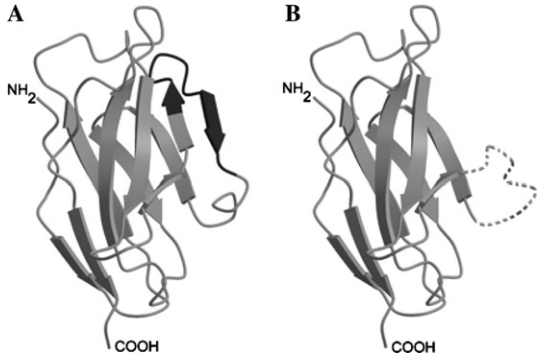

Fig. 2. Comparison of hCD83 versus mCD83 model. (A) The model for the human CD83 was generated on the basis of the Bl-8 Fv fragment (PDB code: 1a6w) using Swiss-Model. Those residues that are absent in murine CD83 are shown in dark gray. (B) Model of the murine CD83, indicating that the global Ig-fold is not affected by the 11-residue deletion. The residues flanking the deletion which cannot reliably be modeled are represented by a dotted line. The figure was generated using the programs Molscript [30] and Raster3D [31].

CD83 is a disulfide-linked homodimeric protein

To investigate if the extracellular domain of CD83 can indeed form homodimers via disulfide bonds, the recombinant human soluble CD83 domain (hCD83ext) was further analyzed using SDS–PAGE analyses under reducing and non-reducing conditions (Fig. 3A) followed by Western blotting using the anti-CD83 antibody CD83-1G11 (Fig. 3B). Interestingly, in the absence of reducing agents, the soluble CD83 molecule formed a dimer, double the size of the monomer (see Figs. 3A, lane 5 and B, lane 4), indicating that all intra- and interchain disulfide bonds are intact. For comparison under reducing conditions, the molecule did not form any dimers anymore (see Figs. 3A, lane 4 and B lane 3).

In order to determine which cysteine residue is responsible for the dimerization of hCD83ext, a mutant form of hCD83ext with a g to c nucleotide transversion which leads to an amino acid exchange of the fifth cysteines at position 129 into a serine residue was cloned (hCD83ext_mut129_CtoS), expressed in *E. coli* and purified, and compared with the hCD83ext wild type protein. As shown in Fig. 3A (lanes 1 and 2) the mutant form of CD83 showed a stable monomeric band under reducing as well as under non-reducing conditions. This band was identical to the hCD83ext wild type protein band analyzed under reducing conditions. The specific-

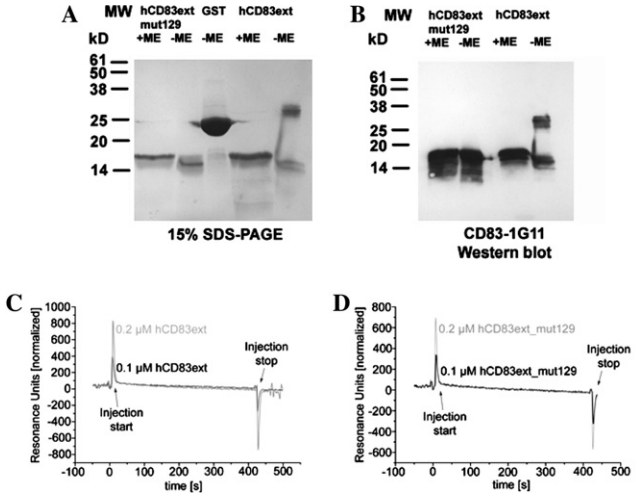

Fig. 3. CD83 is a disulfide-linked homodimer. (A) SDS–PAGE analyses comparing mutant and wild type form of soluble CD83 under reducing (+ME) and non-reducing conditions (−ME). Recombinant human hCD83ext (wild type) and hCD83ext_mut129_CtoS (mutant) protein were analyzed using SDS–PAGE. To identify the possible oligomeric forms of CD83, 2-mercaptoethanol has been omitted from the sample buffer (−ME). GST was used as a control in order to exclude that the upper band is a contamination due to the GST-tag. (B) Western blot analyses using an anti-CD83 specific monoclonal antibody (CD83-1G11). Following the protein separation on a 15% SDS–PAGE, the recombinant proteins were electro-blotted onto nitrocellulose membranes. The specificity of the protein bands was confirmed with the anti-CD83 mAb (CD83-1G11). (C,D) Sensogram analyzing the non-covalent interactions between two hCD83ext or CD83ext and hCD83ext_mut129CtoS molecules. The GST-hCD83ext fusion protein was immobilized on the surface of a CM5 sensor chip. Binding of different concentrations (0.1 and 0.2 μM) of hCD83ext (C) or hCD83ext_mut129CtoS (D) to immobilized hCD83ext was detected by changes in resonance units (RU) over time. The sensograms shown were obtained after reference (GST) subtraction.

ity of the mutant CD83 protein was again confirmed by Western blot analyses (see Fig. 3B, lane 1 and 2). Thus, from these data we conclude that the fifth carboxyterminal cysteine at position 129 of the extracellular CD83 domain is necessary for the formation of homodimers.

In order to investigate if also non-covalent interactions between CD83ext molecules are possible, surface plasmon resonance responses were measured in real time using a Biacore X system. Recombinant GST-hCD83ext was immobilized via anti-GST antibody coupling as ligand onto a CM5 sensor chip. Analytes were different concentrations of hCD83ext or hCD83ext_mut129_CtoS protein diluted in PBS. Data were analyzed with the BIAevaluation program 3.0 (Biacore AB). As shown in Figs. 3C and D, Biacore analyses did not indicate any interactions of hCD83ext with the hCD83ext wild type form (Fig. 3C) or with the mutant hCD83ext_mut129_CtoS monomeric form (Fig. 3D). Under our experimental conditions (RT, PBS) non-covalent CD83 oligomerization was not detectable.

Mutant-monomeric soluble CD83 blocks CD83-expression during DC maturation

Previously we described that the soluble wild type form of CD83 inhibits DC maturation, most prominently it inhibits CD83-expression on the DC during this maturation process [19]. Thus, next we asked if dimerization of CD83 is necessary for this functional property. Immature DC were either incubated with wild type- or with mutant soluble CD83 and at the same time DC-maturation was induced using the maturation cocktail composed of GM-CSF, IL-4, IL-1β, PGE_2, and TNF-α. Cells were incubated for 48 h and then analyzed by FACS. As shown in Fig. 4, both the wild type hCD83ext as well as the mutant CD83 form strongly inhibited the CD83 cell surface expression, while mock or BSA treated cells, which were used as controls, showed a strong upregulation of CD83-expression dur-

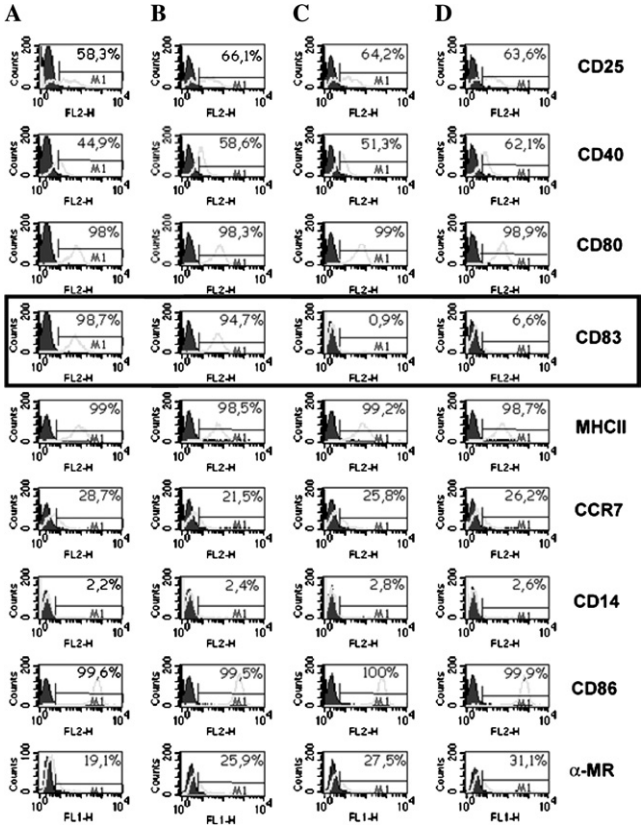

Fig. 4. Monomeric hCD83ext_mut_129_CtoS as well as hCD83ext block CD83-expression during DC maturation. Immature DC were matured in the presence of the maturation cocktail for 48 h (mock control) (A) or in the presence of maturation cocktail plus BSA as a control (10 μg/ml) (B). In addition, immature DC were incubated in the presence of the maturation cocktail in combination with hCD83ext_mut_129_CtoS (10 μg/ml) (C) or in combination with hCD83ext (10 μg/ml) (D). After 48 h the cells were washed and stained with the indicated antibodies and analyzed by FACS. Both hCD83ext as well as hCD83ext_mut129_CtoS strongly reduced the CD83 cell surface expression during DC maturation (frame).

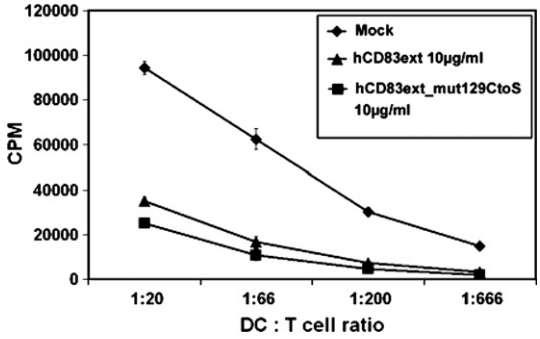

Fig. 5. hCD83ext and the hCD83ext_mut129_CtoS protein inhibit allogeneic T-cell proliferation. MLR analysis: $CD4^+$ and $CD8^+$ human T-cells were stimulated at different ratios with mature allogeneic DC in 96-well plates. These mixed leukocytes were treated with equal concentrations of hCD83ext, hCD83ext_mut129_CtoS, or left untreated (Mock) and incubated for 4 days at 37 °C. Then the cells were pulsed with 1 μCi/well [^{3}H]thymidine (Amersham) for 16 h and analyzed. The hCD83ext_mut129_CtoS mutant showed a slightly better inhibitory effect when compared with the wild type hCD83ext protein. The experiments were performed three times. Data presented here represent a typical experiment.

ing DC maturation. As described before, other cell surface markers typically expressed on mature DC were not influenced by the different soluble CD83 forms.

Inhibition of DC-mediated allogeneic T-cell proliferation using mutant-monomeric soluble CD83

Regarding the functional properties of wild type soluble CD83, we previously reported that it strongly inhibits DC-mediated allogeneic T-cell proliferation. Hence, we studied the inhibitory effect of the mutant-monomeric CD83 protein and compared it with the wild type CD83 protein using a mixed leukocyte reaction (MLR) assay. Interestingly, the mutant CD83 protein inhibited T-cell proliferation slightly better than the soluble wild type protein (see Fig. 5). In addition, the mutant CD83 protein was also analyzed in a murine MLR assay and as previously shown for the wild type form of CD83 [22] also the mutant CD83 protein inhibited the stimulation of murine T-cells very efficiently (data not shown). Thus, in vitro both CD83 isoforms have an impressive immunosuppressive activity.

Discussion

CD83 has been used for a long time as one of the best cell surface markers for mature DC. Recent studies have reported that recombinant soluble CD83 in vitro interferes with DC maturation, cytoskeleton formation and blocks DC-dependent T-cell stimulation [19–21]. In addition, very recently we reported that recombinant soluble CD83 strongly inhibits EAE-associated paralyses, in a prophylactic as well as in a therapeutic setting, and cellular infiltrations in the brain and spinal cord were almost completely blocked [22]. Furthermore, it has been reported by the group of Barry Hock that a soluble form of CD83 is released from activated DC and B-cells, and is detectable in normal human sera [32]. Strikingly, elevated levels of this soluble CD83 molecule have been found in a number of hematological malignancies, suggesting an immunosuppressive role [33].

On the other hand, immobilization of CD83 on the cell surface or overexpression of membrane bound CD83 in cells clearly enhanced T-cell responses [20]. Thus, taken together these data suggest that CD83 plays a dual role: (i) the membrane bound form of CD83 is involved in the induction of cellular immune responses and (ii) while the soluble form of CD83 has strong immunosuppressive properties.

In recent years, several studies have reported about the functional properties of CD83, however nothing has been known regarding the structural properties of this molecule.

Thus, in this study we analyzed the structural properties of CD83. Sequence alignment and domain database searches with hCD83 and mCD83 revealed that the Ig-domain of both proteins comprises the first 108 and 97 residues, respectively, and is connected via a linker sequence with the transmembrane helix. There is an 11-residue deletion comprising residues 65–75 in mCD83. Compared to the sequence of the Bl-8 Fv fragment, which we identified as the closest homologue of known three-dimensional structures, the deletion corresponded to residues in an outer strand of a β-sheet of the hCD83 molecule. It is known from different members of the Ig superfamily that this part of the sequence shows a considerable variability in sequence length and structure without disturbing the Ig core fold. At least for reported inhibitory effects of soluble CD83 this 11-residue deletion has no influence because we could already show that recombinant hCD83ext was also immunosuppressive in the murine system comparable to soluble mCD83ext [22]. Thus, this region could qualify for modifications of CD83 in experimental settings in the future.

Next we took a closer look at the five cysteines, which are located at equivalent sequence positions in hCD83 and mCD83. Two of these positions are highly conserved within the Ig family. CD83 from the nurse shark *G. cirratum* (gCD83), a novel member of the CD83 family, still exhibits a 30% sequence identity to hCD83 and contains three cysteines. Thus, we speculate that an uneven number of cysteines is characteristic for CD83 family members. The remaining cysteine could be used for covalent intermolecular binding with other molecules. To verify this working hypothesis, we analyzed CD83 under reducing and non-reducing conditions, and under the latter experimental conditions the soluble CD83

molecule appeared as a dimer in SDS–PAGE and Western blot analyses. From molecular modeling studies we deduced that the fifth cysteine at amino acid position 129 could be responsible for dimerization. Thus, a mutant form of soluble CD83 was generated having an amino acid exchange from cysteine to serine at this position. And as predicted by the modeling studies this mutant was unable to form dimers, clearly indicating that the fifth cysteine might be responsible for dimerization.

In order to exclude a possible dimerization via non-covalent reactions, the GST-hCD83ext fusion protein was coupled onto CM5 sensor chips, and binding studies with wild type form of soluble CD83 and the mutant form of soluble CD83 were performed using a Biacore X system. Under these experimental conditions no interaction, either between the wild type form or the mutant protein, was detectable. Thus, we conclude that the fifth cysteine residue is indeed responsible for the dimerization of soluble CD83.

Finally, we were able to show that dimerization is not a prerequisite for the immunosuppressive properties of soluble CD83, since DC-mediated T-cell stimulation could be inhibited by the mutant protein at similar levels when compared with the wild type form of soluble CD83.

In summary, here we show for the first time that the soluble form of CD83 forms dimers, however the dimerization is not essential for its immunosuppressive activity, thus also the mutant protein could be used as a therapeutic agent in vivo. This will be investigated in further studies.

Acknowledgments

This work was supported by the Deutsche Forschungsgemeinschaft (SFB466 Grant B5) and by the ELAN Fond (Grant # 03.04.08.1) of the University Hospital of Erlangen.

References

[1] L.J. Zhou, R. Schwarting, H.M. Smith, T.F. Tedder, A novel cell-surface molecule expressed by human interdigitating reticulum cells, Langerhans cells, and activated lymphocytes is a new member of the Ig superfamily, J. Immunol. 149 (1992) 735–742.

[2] E.J. Kozlow, G.L. Wilson, C.H. Fox, J.H. Kehrl, Subtractive cDNA cloning of a novel member of the Ig gene superfamily expressed at high levels in activated B lymphocytes, Blood 81 (1993) 454–461.

[3] M. Lechmann, E. Kremmer, H. Sticht, A. Steinkasserer, Overexpression, purification, and biochemical characterization of the extracellular-human CD83 domain and generation of monoclonal antibodies, Protein Expr. Purif. 24 (2002) 445–452.

[4] C.J. Twist, D.R. Beier, C.M. Disteche, S. Edelhoff, T.F. Tedder, The mouse CD83 gene: Structure, domain organization, and chromosome localization, Immunogenetics 48 (1998) 383–393.

[5] S. Berchtold, P. Mühl-Zürbes, C. Heufler, P. Winklehner, G. Schuler, A. Steinkasserer, Cloning, recombinant expression and biochemical characterization of the murine CD83 molecule which is specifically upregulated during dendritic cell maturation, FEBS Lett. 461 (1999) 211–216.

[6] D. Weissman, Y. Li, J. Ananworanich, L.J. Zhou, J. Adelsberger, T.F. Tedder, M. Baseler, A.S. Fauci, Three populations of cells with dendritic morphology exist in peripheral blood, only one of which is infectable with human immunodeficiency virus type 1, Proc. Natl. Acad. Sci. USA 31 (1995) 826–830.

[7] L.J. Zhou, T.F. Tedder, Human blood dendritic cells selectively express CD83, a member of the immunoglobulin superfamily, J. Immunol. 15 (1995) 3821–3835.

[8] L.J. Zhou, T.F. Tedder, $CD14^{+}$ blood monocytes can differentiate into functionally mature $CD83^{+}$ dendritic cells, Proc. Natl. Acad. Sci. USA 93 (1996) 2588–2592.

[9] R.M. Steinman, The dendritic cell system and its role in immunogenicity, Annu. Rev. Immunol. 9 (1991) 271–296.

[10] J. Bancherau, R.M. Steinman, Dendritic cells and the control of immunity, Nature 392 (1998) 245–252.

[11] J. Bancherau, F. Briere, C. Caux, J. Davoust, S. Lebecque, Y.J. Liu, B. Pulendran, K. Palucka, Immunobiology of dendritic cells, Annu. Rev. Immunol. 18 (2000) 767–811.

[12] M. Kruse, O. Rosorius, F. Kratzer, G. Stelz, C. Kuhnt, G. Schuler, J. Hauber, A. Steinkasserer, Mature dendritic cells infected with Herpes Simplex virus type 1 exhibit inhibited T-cell stimulatory capacity, J. Virol. 74 (2000) 7127–7136.

[13] S.C. Knight, S. Paderson, Bone marrow-derived dendritic cells infection with human immunodeficiency virus and immunopathology, Annu. Rev. Immunol. 15 (1997) 593–615.

[14] I. Fugier-Vivier, C. Servet-Delprat, P. Rivailler, M.C. Riossan, Y.J. Liu, C. Rabourdin-Combe, Measle virus suppresses cell-mediated immunity by interfering with the survival and functions of dendritic and T cells, J. Exp. Med. 186 (1997) 813–823.

[15] J. Engelmayer, M. Larson, M. Subklewe, A. Chahroudi, W.I. Cox, R.M. Steinman, N. Bhardwaj, Vaccinia virus inhibits the maturation of human dendritic cells: A novel mechanism immune evasion, J. Immunol. 163 (1999) 6762–6768.

[16] L. Jenne, G. Schuler, A. Steinkasserer, Viral vectors for dendritic cell-based immunotherapy, Trends Immunol. 22 (2001) 102–107.

[17] B. Senechal, A.M. Boruchov, J.L. Reagan, D.N. Hart, J.W. Young, Infection of mature monocyte-derived dendritic cells with human cytomegalovirus inhibits stimulation of T-cell proliferation via the release of soluble CD83, Blood 103 (2004) 4207–4215.

[18] M. Kruse, O. Rosorius, F. Kratzer, D. Bevec, C. Kuhnt, A. Steinkasserer, G. Schuler, J. Hauber, Inhibition of CD83 cell surface expression during dendritic cell maturation by interference with nuclear export of CD83 mRNA, J. Exp. Med. 191 (2000) 1581–1590.

[19] M. Lechmann, D.J.E.B. Krooshoop, D. Dudziak, E. Kremmer, C. Kuhnt, C.G. Figdor, G. Schuler, A. Steinkasserer, The extracellular domain of CD83 inhibits dendritic cell-mediated T cell stimulation and binds to a ligand on dendritic cells, J. Exp. Med. 194 (2001) 1813–1821.

[20] N. Scholler, M. Hayden-Ledbetter, A. Dahlin, I. Hellstrom, K.E. Hellstrom, J.A. Ledbetter, CD83 regulates the development of cellular immunity, J. Immunol. 168 (2002) 2599–2602.

[21] N. Kotzor, M. Lechmann, E. Zinser, A. Steinkasserer, The soluble form of CD83 dramatically changes the cytoskeleton of dendritic cells, Immunobiology 209 (2004) 129–140.

[22] E. Zinser, M. Lechmann, A. Golka, M. Lutz, A. Steinkasserer, Prevention and treatment of experimental autoimmune encephalomyelitis (EAE) by soluble CD83, J. Exp. Med. 200 (2004) 345–351.

[23] S.F. Altschul, T.L. Madden, A.A. Schäffer, J. Zhang, Z. Zhang, W. Miller, D.J. Lipman, Gapped BLAST and PSI-BLAST: A

new generation of protein database search programs, Nucleic Acids Res. 25 (1997) 3389–3402.
[24] A. Bateman, E. Birney, L. Cerruti, R. Durbin, L. Etwiller, S.R. Eddy, S. Griffiths-Jones, K.I. Howe, M. Marshall, E.L. Sonnhammer, The Pfam protein families database, Nucleic Acids Res. 30 (2002) 276–280.
[25] J. Schultz, F. Milpetz, P. Bork, C.P. Ponting, SMART, a simple modular architecture research tool: Identification of signaling domains, Proc. Natl. Acad. Sci. USA 95 (1998) 5857–5864.
[26] K. Karplus, R. Karchin, C. Barrett, S. Tu, M. Cline, M. Diekhans, L. Grate, J. Casper, R. Hughey, What is the value added by human intervention in protein structure prediction? Proteins Suppl. 5 (2001) 86–91.
[27] N. Guex, M.C. Peitsch, SWISS-MODEL and the Swiss-Pdb-Viewer: An environment for comparative protein modelling, Electrophoresis 18 (1997) 2714–2723.
[28] R.W.W. Hooft, G. Vriend, C. Sander, E.E. Abola, Errors in protein structures, Nature 381 (1996) 272.
[29] Y. Ohta, E. Landis, T. Boulay, R.B. Phillips, B. Collet, C.J. Secombes, M.F. Flajnik, J.D. Hansen, Homologous of CD83 from Elasmobranch and Teleost fish, J. Immunol. 173 (2004) 4553–4560.
[30] P. Kraulis, Molscript: A program to produce both detailed and schematic plots of protein structures, J. Appl. Crytallogr. 24 (1991) 946–950.
[31] E.A. Merritt, M.E.P. Murphy, Raster3D version 2.0 a program for photorealistic molecular graphics, Acta Crystallogr. 50 (1994) 869–873.
[32] B.D. Hock, M. Kato, J.L. McKenzie, D.N. Hart, A soluble form of CD83 is released from activated dendritic cells and B lymphocytes, and is detectable in normal human sera, Int. Immunol. 13 (2001) 959.
[33] B.D. Hock, L.F. Haring, A. Steinkasserer, K.G. Taylor, W.N. Patton, J.L. McKenzie, The soluble form of CD83 is present at elevated levels in a number of hematological malignancies, Leukemia Res. 28 (2004) 237–241.